ICES Journal of Marine Science, 2024, Vol. 82, Issue 5, fsae188
https://doi.org/10.1093/icesjms/fsae188
Received: 8 October 2024; **revised:** 7 December 2024; **accepted:** 9 December 2024
Original Article

Exploring the role of body mass in temperature-driven changes in metabolic rates of Arctic copepods

Konrad Karlsson [1,2,*] **and Janne E. Søreide** [2]

[1]Department of Aquatic Resources, Institute of Freshwater Research, Swedish University of Agricultural Sciences, Stångholmsvägen 2, SE-178 93 Drottningholm, Sweden
[2]Arctic Biology, Svalbard Science Centre, The University Centre in Svalbard, PO Box 156, N-9171 Longyearbyen, Norway

*Corresponding author. Department of Aquatic Resources, Institute of Freshwater Research, Swedish University of Agricultural Sciences, Stångholmsvägen 2, SE-178 93 Drottningholm, Sweden. E-mail: Konrad.karlsson@slu.se

Abstract

As Arctic sea temperatures rise and sea ice declines, boreal species are becoming more abundant in these waters. Generally, both inter- and intra-species variations show larger body sizes at higher latitudes and in colder climates. Continued Arctic amplification may lead to shifts in the size and composition of marine plankton, with cascading effects throughout the ecosystem. This study examines the metabolic rates of three common zooplankton species, *Calanus finmarchicus*, *C. glacialis*, and *Metridia longa*, across different temperatures (0°C, 3°C, and 6°C) to understand these dynamics. Results showed a distinct decrease in aerobic scope with rising temperatures for all three copepod species, indicating potential fitness reductions in warmer waters. Larger copepods exhibited higher aerobic scopes than smaller ones at all temperatures; however, this advantage diminished at 6°C, suggesting that smaller body sizes may confer metabolic benefits at higher temperatures. Conversely, larger sizes are favored in colder waters. These findings help explain the increase of smaller boreal species in warming Arctic seas and why colder Arctic conditions favor larger individuals.

Keywords: aerobic scope; invertebrates; copepods; physiology; climate change; warming

Introduction

Temperature is a key predictor of metabolic rate and determines the range limit and abundance of species. Metabolic rate, a measure of energy used by an organism per unit of time, is largely influenced by temperature and activity level. The intense warming of the Arctic, known as Arctic amplification, which contributes to sea ice loss and significant ocean warming, will impact the Arctic marine ecosystem (Renaud et al. 2018, Griffith et al. 2019). A key question is how plankton communities will respond physiologically and consequently restructure due to increased sea temperatures. There is no clear consensus on how to interpret the effects of temperature on metabolic rates in terms of fitness, such as growth, reproduction, and survival (Pörtner 2001, Pörtner and Farrell 2008, Lefevre 2016, Jutfelt et al. 2018). Within a temperature range that is not directly harmful to an organism, predicting the organism's optimal temperature is challenging. This is partly because metabolic rates are plastic, and the advantage of having relatively low or high rates depends on the context (Burton et al. 2011); low rates are beneficial for conserving energy, while high rates are advantageous for growth and reproduction if resources are sufficient. Therefore, it is difficult to determine what metabolic rate implies in terms of fitness without considering the context of the organisms' life history and surrounding environment.

It has been suggested that the difference between maximum (an active animal) and minimum metabolic rates (an animal at rest), known as aerobic scope, can indicate a species' temperature preferences (Pörtner and Farrell 2008). The greater the aerobic scope, the higher the species' performance or fitness. Therefore, within a range of temperatures, the temperature with the greatest aerobic scope is considered the most optimal for the organism (Pörtner and Farrell 2008). One theory posits that the fitness of aquatic ectotherms scales with aerobic scope, as it represents metabolic performance above maintenance levels (i.e. above minimum metabolic rate) and indicates how much of the animal's metabolism can be allocated to fitness-enhancing activities such as growth, reproduction, and behavior (Pörtner 2001, Pörtner and Farrell 2008). The framework of partitioning metabolic rate across temperatures provides a practical approach to investigate the effects of warming on aquatic ectotherms (Rubalcaba et al. 2020, McKenzie et al. 2021). However, this approach is not always straightforward; in some organisms, the greatest aerobic scope may occur near lethal temperatures, and aerobic scope can also be higher outside the organism's natural temperature range (Lefevre 2016, Jutfelt et al. 2018).

There are many definitions and terms used to describe the different levels of metabolic rates expressed by a single individual (e.g. Burton et al. 2011, Clark et al. 2013, Morozov et al. 2018). Here, we define resting metabolic rates (RMR) as the rates of an inactive organism with no ongoing digestion (Karlsson and Søreide 2023). In contrast, active metabolic rates (AMRs) are expressed by an individual that performs strenuous activity, such as escaping a predator (or being handled by a researcher), or during the digestion of large meals (Skjoldal et al. 1984, Clark et al. 2013, Karlsson and Søreide 2023).

Some definitions of metabolic rate are highly stringent, focusing on the absolute lowest or highest rates an individual

can express, i.e. the "true" minimum and maximum rates (Fry 1971, Clark et al. 2013). While such rigor is theoretically ideal, it can hinder practical research. Our definitions are more flexible, accounting for spontaneous individual variation in resting and AMRs. We recognize that such variation is an estimable source of error that can ultimately enhance the reliability of conclusions. Instead, we prioritize designing experiments where the environment is standardized and predictable for all organisms (Falconer and Mackay 1996).

Since metabolic rate is a fitness trait, it can be used to investigate temperature tolerance and compare temperature adaptations between species and populations. Variation in fitness traits is a key component of adaptation, where genetic variation within a population is linked to its adaptive potential (Falconer and Mackay 1996, Karlsson and Winder 2020). This potential for adaptation in metabolic rate is subject to natural selection, leading to differentiation between populations or species and resulting in local adaptation (Falconer and Mackay 1996, Karlsson and Winder 2020). Consequently, it is likely that species or populations from colder areas are less tolerant of higher temperatures than those from warmer areas, and vice versa (Seth et al. 2013). This suggests that boreal species may benefit from increasing Arctic Sea temperatures, potentially expanding their range and numbers at the expense of Arctic species (Gluchowska et al. 2016, Weydmann et al. 2017).

The effect of temperature on metabolic rate is mass-dependent, with larger individuals experiencing a greater increase in metabolic rate as temperature rises (Fossen et al. 2019). Additionally, the reduction in aerobic scope is more pronounced in larger individuals compared to smaller ones, causing larger individuals to lose relatively more fitness as temperatures increase (Rubalcaba et al. 2020). Consequently, warming can influence both inter- and intra-species composition among individuals of different sizes, leading to cascading effects on population and community structures (Lindmark et al. 2018). Understanding size-temperature interactions is therefore crucial for predicting how warming will affect populations, especially in the Arctic, where copepods tend to be larger than those in boreal regions (Renaud et al. 2018).

The aim of this study is to determine the effect of temperature and body mass on the metabolic rate of three common Arctic zooplankton species. The mesozooplankton communities in the Arctic and Sub-Arctic Seas are dominated by calanoid copepods, with *Calanus finmarchicus*, *C. glacialis*, and *Metridia longa* being three of the most abundant species (Daase et al. 2008). These three copepod species largely co-occur in the European Arctic but have different geographic distribution preferences. The largest of the three, *C. glacialis*, is a distinctly Arctic species, while the slightly smaller *C. finmarchicus* is a boreal species transported northwards to Svalbard and the Arctic Ocean by the warmer North Atlantic currents (Choquet et al. 2017). The smallest species, *M. longa*, has the largest geographical distribution, completely overlapping the range of the two *Calanus* species, but is more abundant in oceanic, Atlantic-influenced seas (size and geographic range distribution shown in Fig. 1a–c; source: Klekowski and Węsławski 1991).

Metabolism depends on organisms' feeding and life strategies (Hagen 1999). The three species are omnivorous filter feeders but primarily rely on phytoplankton when available. The two *Calanus* species create a current that draws in particles suspended in the water column, while *M. longa* is a

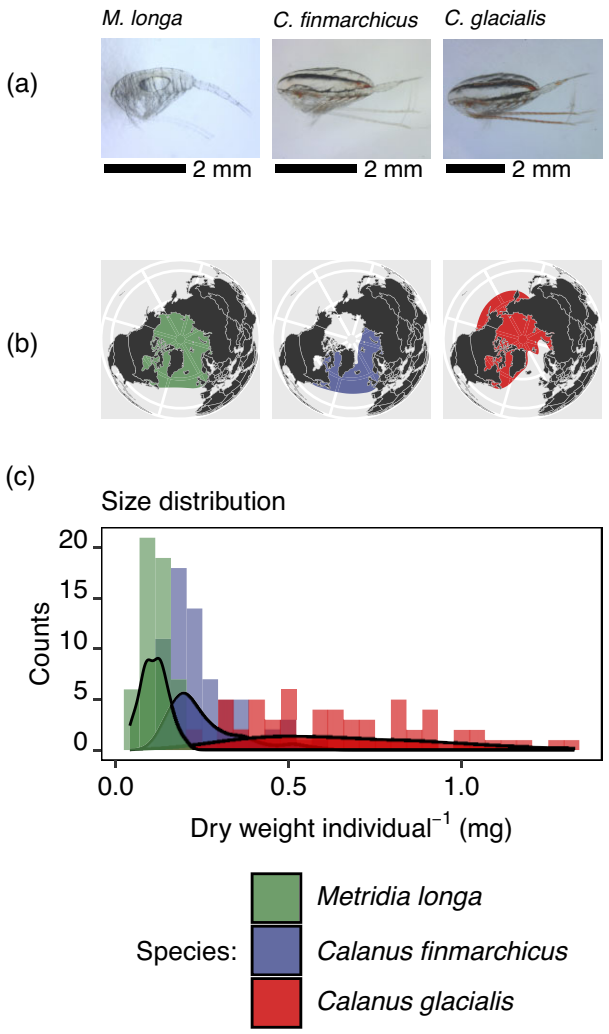

Figure 1. Photos in panel (a) show how the copepod species appear under a microscope at 1.6x magnification, lying on their right side. The photos have been cropped, and a 2 mm scale bar is added below each photo for reference. All individuals were of the copepodid stage 5 (C5) developmental stage, which is the last stage before becoming adults. Panel (b) displays the distribution maps of the three copepod species, where *Metridia longa* has the widest distribution, overlapping with the ranges of both *Calanus finmarchicus* and *C. glacialis*. *C. finmarchicus* generally has a more southern distribution range, while *C. glacialis* has a more northern pan-Arctic distribution range (Klekowski and Węsławski 1991). Panel (c) presents the size distributions of the three calanoid copepod species included in this study. *M. longa* is the smallest, *C. finmarchicus* is intermediate in size, and *C. glacialis* is the largest. The size distribution in panel (c) is depicted both as a frequency histogram and as a kernel density estimate, which provides a smoothed version of the histogram.

cruise feeder and actively swims through the water column while creating a feeding current and intercepting food (Kiørboe 2011). The *Calanus* species store large amounts of fat and enter dormancy to sustain themselves during the long dark winter without feeding (Falk-Petersen et al. 2009, Clark et al. 2012). The *Calanus* winter dormancy is commonly termed diapause, but individuals are not so dormant that they stop responding to external cues (Coguiec et al. 2023), e.g. individuals still flee from a pipette upon capture. However, other cues, such as temperature and food that would under other circumstances trigger activity, may have reduced or no effect

(Hopkins et al. 1984, Ingvarsdóttir et al. 1999, Morata and Søreide 2015). In contrast to the *Calanus* species, *M. longa* store less fat and remain active throughout the winter, feeding opportunistically (Hopkins et al. 1984). Independent of their body sizes, we therefore expected different metabolic rates due to their varying life histories and activity levels (Karlsson and Søreide 2023).

The size range of copepods in this study presents more than a 30-fold difference in body mass (Fig. 1c), providing an opportunity to investigate the interactive effects of mass and temperature. As warming is expected to have more adverse effects on larger organisms than on smaller ones, we anticipated a reduction in aerobic scope with size due to increasing RMRs with increasing body mass (Rubalcaba et al. 2020). Furthermore, based on their geographic preferences, we expected *C. glacialis* to have a narrower aerobic scope at higher temperatures, as this species is primarily exposed to lower temperatures, making it theoretically less tolerant to higher temperatures compared to the other two (Fig. 1b).

Materials and methods

Sampling

Sampling took place in Isfjorden, a large fjord with several side arms located in West Spitsbergen (Fig. 2). Three locations in Isfjorden were sampled during the autumn of 2020, from 14 September to 2 October: the inner part, Billefjorden (BAB, 78.65°N, 16.658°E); the central part, Karlskronadjupet (ISK, 78.321°N, 15.163°E); and the outer part, close to Grønfjorden (ISG, 78.129°N, 14.003°E). The fauna becomes progressively more Atlantic, and the water temperature warmer, further out in Isfjorden and closer to the shelf break near the West Spitsbergen Current (WSC), which brings warm Atlantic water to the Arctic (Skogseth et al. 2020). Temperatures in Isfjorden range between −1.8°C and 6°C during summer and between −1.8°C and 1.5°C during winter (Skogseth et al. 2020). In Billefjorden, the innermost part of Isfjorden, two shallow sills prevent warm, dense Atlantic water origin from the WSC to enter. Sea temperatures around −1°C persist year-round below 100 m depth in Billefjorden (Skogseth et al. 2020, Søreide et al. 2022). Here, *C. glacialis* strongly dominates (>90%) over *C. finmarchicus* (Arnkværn et al. 2005, Gabrielsen et al. 2012), while the two *Calanus* species are present in more comparable numbers in the central and outer parts of Isfjorden (Gluchowska et al. 2016, Hatlebakk et al. 2022). The oceanic *M. longa* is generally scarce in the fjord's inner parts but becomes increasingly abundant closer to the Atlantic waters of the Fram Strait (Diel 1991, Gluchowska et al. 2016). Consequently, *M. longa* could not be sampled in Billefjorden, as their numbers were too low here.

Samples were collected using a WP3 net with a 1 m^2 opening and 1 mm mesh size (UNESCO 1968), hauled vertically from 20 m above the seafloor to the surface. (Station depths were 191, 274, and 272 m for BAB, ISK, and ISG, respectively.) Immediately after the haul, the animals were gently transferred to 30 l buckets filled with ambient seawater. Once in the laboratory, the animals were further diluted with ambient water in 100 l buckets and kept in a cold room at 0°C. The primary objective during storage was to maintain the animals' health by ensuring high water quality, which involved daily checks for foul odors and the removal of gelatinous and macro-zooplankton from the buckets.

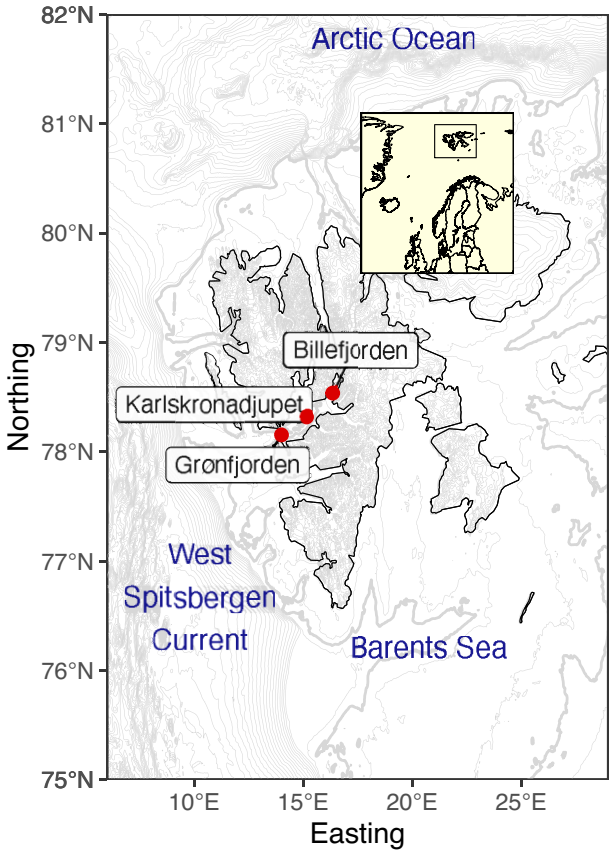

Figure 2. Bathymetric map of Svalbard illustrating the locations of the three sampling stations in Isfjorden. Black lines indicate the borders between water and land, while gray lines show elevation. The inset map displays the location of the Svalbard Islands north of Scandinavia. Bathymetric data were sourced from the "marmap" package (Pante et al. 2023) and plotted using the "sf" and "ggplot2" packages (Wickham 2016, Pebesma and Bivand 2023).

Experimental setup and measurements of metabolic rates

We investigated the effect of temperature on metabolic rate at 0°C, 3°C, and 6°C (Table 1). All individuals were juvenile copepods at the copepodid stage 5 (C5), the final juvenile stage before adulthood. The C5 was identified by counting the number of segments on the urosome, following the description provided by Klekowski and Węsławski (1991). By exclusively using copepods at the C5 developmental stage, we eliminated variance due to life stage, which can influence metabolic rate (Karlsson and Søreide 2023). The main reasons for using C5 copepods in this experiment were that they are highly abundant during this part of the season in comparison to adults; meanwhile, they are sufficiently large, and hence, individually consume enough oxygen to be detected by our instruments.

Since adaptation and acclimatization may occur along the temperature gradient in Isfjorden (Skogseth et al. 2020), we used 179 individuals from three locations along this gradient and included location as a covariate in our analyses. Additionally, each individual was incubated three to four times at each temperature (Table 1), allowing us to cross each individual over the temperature range. This approach ideally results in more accurate measurements of temperature effects by controlling for individual variation (Bolker et al. 2009). Con-

Table 1. Number of sampled individuals per species and sampling station in Isfjorden, Svalbard.

Species	Sampling station	Number of individuals	Measurements at 0°C	Measurements at 3°C	Measurements at 6°C
C. finmarchicus	BAB	17	204 (4)	204 (4)	204 (4)
C. glacialis	BAB	20	234 (4)	240 (4)	240 (4)
M. longa	BAB	0	–	–	–
C. finmarchicus	ISK	32	288 (3)	288 (3)	288 (3)
C. glacialis	ISK	20	180 (3)	180 (3)	180 (3)
M. longa	ISK	19	171 (3)	171 (3)	171 (3)
C. finmarchicus	ISG	18	162 (3)	162 (3)	159 (3)
C. glacialis	ISG	19	171 (3)	171 (3)	171 (3)
M. longa	ISG	34	306 (3)	306 (3)	306 (3)

Calanus finmarchicus and *C. glacialis* were the only species present in Billefjorden (BAB), the innermost part of Isfjorden. In contrast, all three species, including *M. longa*, were found at Karlskronadjupet (ISK) in the central part of Isfjorden, and at Grønfjorden (ISG) near the fjord's mouth, bordering the WSC (warm Atlantic water). *Metridia longa* was absent at BAB, so additional individuals were sampled at ISG to make the sample sizes of each species comparable. The measurement columns display the total number of measurement series, which includes individual × repeated measurements × type of measurement (AMR, RMR, and aerobic scope) per temperature and station. The number of repeated measurements per individual is shown in parentheses. Initially, there were four repeated measurement series, but this was later reduced to three as four were deemed excessive.

sequently, individual identity was used as a random effect in our analyses. We also included the number of repeated measurements, ranging from 1 to 4, as a covariate, as repeated measurements may affect the metabolic rate data. This was done to estimate the variation that could result from repeated handling of both the instrument and the copepods.

Oxygen measurements were taken using a sensor dish reader (microplate system from Loligo®). This optical instrument measures oxygen concentration from sensor spots (e.g. Karlsson and Søreide 2023). A transparent glass dish with 24 wells is placed on top of the dish reader. Each well contains a sensor spot, enabling the simultaneous reading of 24 oxygen concentrations. Twenty wells per dish were used for copepods, while four wells containing only seawater served as controls to measure background respiration. Two sensor dish readers operated simultaneously, allowing 40 individual measurements at a time.

Just before the experiment, the copepods were gently sieved out of their large holding tanks into a shallow tray containing ∼2 cm of seawater. To keep the copepods cold, the tray was placed on ice, and the initial sorting before the experiments was conducted in a cold room at 6°C. From the tray, copepods were selected one by one using a pipette and transferred into a bowl of 0.45 μm filtered, air-saturated seawater at 0°C. This intermediate step reduced the risk of introducing other organisms into the wells. The copepods were then pipetted into the wells of the glass plate, each filled with 500 μl of air-saturated, 0°C seawater filtered through a 0.45 μm filter. Each well, except the empty control wells, contained one copepod. The wells were sealed from the air with silicone padding, held in place by a heavy plastic-coated metal plate. The glass dishes were placed on the sensor dish readers, which were in turn placed in an incubator set to the experimental temperature. All experiments began at 0°C, the holding temperature, and were gradually increased in increments of 3°C to a maximum of 6°C.

Between repeated measurements, the copepods remained in their wells while the seawater from the previous temperature experiment was removed with a pipette. Enough water was left in the well to prevent the copepod from drying out, and the wells were then refilled with an excess of air-saturated water, forming a cap over the wells. This procedure of removing and adding seawater was repeated twice before the wells were sealed again. Thus, the water in the wells was completely changed between measurements without removing the copepods. The filtered seawater used in the experiments was kept inside the same incubator where the experiments took place and was continuously aerated with air stones.

Between temperature changes, the copepods remained in their wells inside the incubator overnight to acclimatize to the 3°C increase. The temperature was always increased in increments of 3°C from the initial 0°C (0°C, 3°C, and 6°C). For an individual copepod, the entire experiment typically concluded within 3 days, with one temperature treatment per day. When logistical constraints prevented consecutive lab work, the experiments took longer, though this was the exception. After the experiments, the copepods were photographed and placed in pre-weighed tin cups. They were then freeze-dried at −50°C and 0.2 mbar for at least 12 h in a LABCONCO FreeZone tray dryer. The copepods were then weighed on a Mettler-Toledo XPR microbalance with 0.001 mg readability. The dry weight of the copepods was used as a covariate in the analyses of metabolic rate.

Data handling

The statistical software R was used for data handling and analysis. Oxygen measurements ranged from 39 to 76 min (more than half of the measurements were 76 min long), and readings were taken every 5 s. For each individual measurement, an asymptotic curve was fitted to the raw data using a linear regression model that expressed the change in phase value as a function of time, incorporating both a linear and logarithmic term: phase = time + e^{time}. Predictions and extrapolations of the fitted curves were extended to 76 min to ensure that all curves were of equal length. Each curve was then interpolated to have a predicted phase value every 15 s, ensuring uniformity in length and data points across curves. The phase values were converted to oxygen concentrations using the calibration values of the sensor spots. The relationship between phase values and oxygen concentration is linear, so a two-point calibration with oxygen-depleted and oxygen-saturated seawater was performed to determine the corresponding phase value-to-oxygen ratio (Karlsson and Søreide 2023). This calibration was conducted for each of the three temperatures, as the oxygen concentration of air-saturated seawater decreases with temperature (349, 323, and 300 μmol l^{-1} at 0°C, 3°C, and 6°C, respectively).

For every 24 readings per dish, there were four control wells. The average oxygen concentration of these control wells

was calculated for each time point i (in 15-s increments). The next step was to calculate the difference between the starting oxygen concentration and the concentration at time i. Ideally, the control wells should maintain the same oxygen concentration throughout the experiment, resulting in a flat line. However, due to background respiration and sensor drift, this was not the case. To account for these factors, the difference in oxygen concentration in the control wells at time i was added to the oxygen concentrations measured in the wells with copepods. This adjustment was made to remove changes in oxygen levels that were not caused by the copepods' metabolic rates. The oxygen concentration from the control was added because the oxygen curve in the wells with copepods was artificially steepened by background respiration and sensor drift. Adding the oxygen flattens the curve, correcting for these artifacts. Alternatively, if the correction had been applied to the metabolic rates, the control rates would have been subtracted from the copepod rates.

After adjusting for control oxygen levels, the data were analyzed using rolling regressions fitted with the R "zoo" package (Zeileis and Grothendieck 2005). This method estimates a regression coefficient for each 5-min interval along the curve, continuing until <5 min remain, at which point the analysis terminates. In other words, the regression is calculated from points $i, i+1, \ldots$ up to the end of the time window.

The rolling regression analysis produced 286 coefficients of metabolic rate per repeated measurement. AMR and RMR were estimated from these values using density estimation with the R package "mclust" (Scrucca et al. 2023). At the beginning of each measurement, the copepods were agitated by the handling procedure, leading to initially higher metabolic rates that decreased over time (Karlsson and Søreide 2023). These elevated rates were identified as AMR, while the later lower rates were considered RMR. Various definitions and terms exist for measuring metabolic rate (e.g. Burton et al. 2011, Clark et al. 2013, Morozov et al. 2018). The key to our experiments is that the environment was consistent and controlled, allowing for comparisons of individuals within this study in a common setting (Falconer and Mackay 1996).

The function "densityMclust" in the "mclust" package performs cluster analysis and estimates a set of probability density distributions for the observed normally distributed data. Since the activity level of the animals is unknown, this analysis assumes that both AMR and RMR for each individual are measured with normally distributed errors (Chabot et al. 2016). The means of these normal distributions were taken as point estimates for AMR and RMR. Finally, subtracting RMR from AMR yields the aerobic scope, which can serve as a potential fitness metric (Pörtner and Farrell 2008). Thus, three estimates were obtained for each individual during each repeated measurement: AMR, RMR, and aerobic scope.

The original units of μmol O_2 l^{-1} min^{-1} were converted to μmol O_2 day^{-1} by appropriately scaling to the volume of water in the well and multiplying by 60 (min) × 24 (h).

Mixed model analysis

Metabolic rate (μmol O_2 day^{-1}) was analyzed using a mixed model implemented with the "lmer" function from the lme4 package (Bates et al. 2015). The model was structured to address our experimental hypotheses (Equation 1). We examined the effect of body mass on metabolic rate across different temperatures through a three-way interaction involving mass, type of metabolic measurement (three levels: AMR, RMR, and aerobic scope), and temperature (continuous variable: 0°C, 3°C, and 6°C). Additionally, the species-specific rates across temperatures were analyzed through a three-way interaction between species (three levels: *C. finmarchicus*, *C. glacialis*, and *M. longa*), type of metabolic measurement, and temperature.

Additionally, the effects of sampling station (three levels: BAB, ISG, and ISK), repeated measurement (continuous variable: 1, 2, 3, and 4), and measurement time (continuous variable: ranging from 39 to 75 min) were included in the model. Both metabolic rate and mass were log-transformed to reduce heteroscedasticity and account for the non-linearity between rate and body mass. Model effects were calculated as partial regressions using the "effects" package and plotted with the "ggplot2" and "patchwork" packages (Wickham 2016, Fox and Weisberg 2018, 2019, Pedersen 2023). The "lmer" model formula was specified as follows:

$$\begin{aligned}\log(\text{metabolic rate}) \sim\ & \text{station} + \text{repeated measurement} \\ & + \text{measurement time} + \log(\text{dry weight}) \\ & \times \text{metabolic measurement} \times \text{temperature} \\ & + \text{species} \times \text{metabolic measurement} \times \text{temperature} \\ & + (\text{temperature}|\text{species} : \text{unique ID}).\end{aligned} \quad (1)$$

In the above log–log regression, both the independent variable dry weight and the dependent variable metabolic rate are logged. Back-transforming these predictions would involve exponentiating both variables. This approach can sometimes lead to biased interpretation of the summary statistics of the linear model compared to the original scale estimates. Hence, we do not present P-values from this model. Instead, confidence intervals presented in the figures were used to assess "significance."

Time-specific analysis of metabolic data

The rolling regression analysis produced 286 coefficients of metabolic rate per repeated measurement, each regression was calculated using data points collected at 15-s intervals, spanning a 5-min rolling window from time 0 to 71.5 min, i.e. 71.5/0.25 = 286. After 71.5 min, the analysis terminated as the regression exceeded the available data bounds. For each of our 179 individuals (Table 1), we calculated the mean metabolic rate of the repeated measurements at time i at each temperature. Resulting in a data frame of 286 (time) × 179 (individuals) × 3 (temperature) = 153 582 observations of metabolic rate.

This data frame was split by time, producing 286 smaller data frames, each containing time-specific measurements of metabolic rate. While metabolic rate values were unique to each time frame, variables such as species, temperature, and dry weight remained constant across data frames. Using these time-specific data frames, we fit identical linear regression models to evaluate the explanatory power of different variables (species, temperature, and dry weight) for metabolic rate over time.

By using the built-in R function "lapply," we fitted 286 linear models and extracted the adjusted R^2 values. Each model used log-transformed metabolic rate as the response variable, and the explanatory variables included log-transformed dry weight, temperature, and species. Five model sets were fitted: (1) all variables (species, temperature, and dry weight), (2) dry weight only, (3) species only, (4) temperature only, and (5) a null model (intercept only).

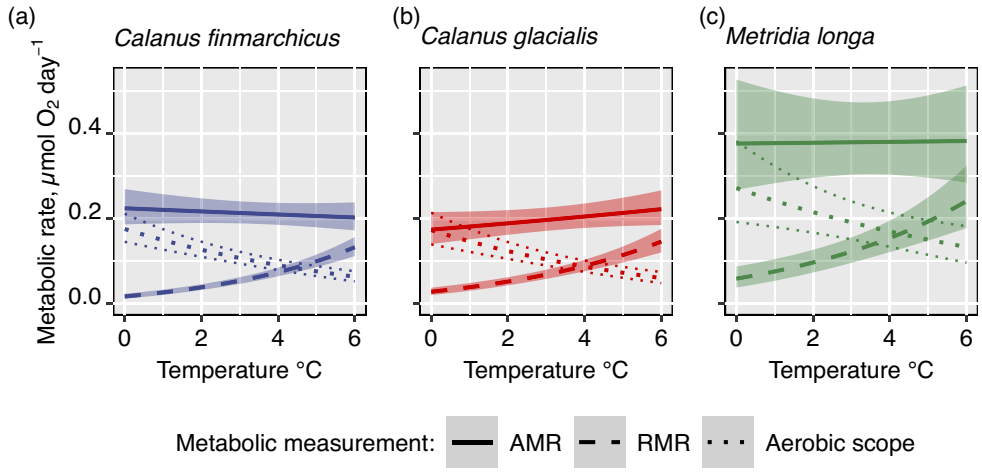

Figure 3. Model effects (partial regressions) from the three-way interaction between temperature, species, and metabolic measurement for *C. finmarchicus* (a), *C. glacialis* (b), and *M. longa* (c). The 95% confidence intervals are represented as shaded ribbons for AMR and RMR, and as dots for aerobic scope. The AMR is depicted by a solid line, the RMR by a dashed line, and the aerobic scope by a dotted line. Partial regression predictions were calculated by setting the remaining predictors (i.e. all but temperature, species, and metabolic measurement) to their average value (Fox and Weisberg 2018).

In addition, we calculated the average metabolic rate over time for each temperature and species. For temperature, we first averaged repeated measurements per individual at each time point, then calculated the average across all individuals at each temperature and time. For species, we averaged across temperature treatments at each time point for individuals within each species.

Genetic species identification of *Calanus*

There is no consensus on how to visually distinguish between *C. finmarchicus* and *C. glacialis*, as the two species are morphologically very similar (Choquet et al. 2018). However, we used red pigmentation in the urosome to differentiate between the species before the experiment, based on insights from a previous study where red pigmentation was observed only on the urosome of *C. glacialis* (see Fig. 2a and b in Karlsson and Søreide 2023). After the experiment, the species of *Calanus* were genetically identified as described by Karlsson and Søreide (2023), using a DNA extraction technique outlined by Montero-Pau et al. (2008) and primers described by Smolina et al. (2014). The genetic analysis confirmed that all individuals were correctly classified based on the red pigmentation of the urosome.

Results

The three-way interaction between species, temperature, and metabolic measurement revealed contrasting metabolic rates across species (Fig. 3a–c). *Metridia longa* exhibited higher AMRs and a greater aerobic scope compared to *C. finmarchicus* and *C. glacialis*. Generally, AMRs remained fairly constant across temperatures for all species, while RMRs steadily increased with temperature, thereby reducing the aerobic scope.

The three-way interaction between dry weight, temperature, and metabolic measurement showed that AMRs increased with dry weight but were relatively consistent across temperatures and, hence, were not significantly affected by the interaction between temperature and dry weight (Fig. 4a–c). In contrast, RMRs increased more with dry weight at 6°C than at 0°C. This led to a greater increase in aerobic scope with increasing dry weight at 0°C than at 6°C.

The three main effects—sampling station (Fig. 5a), repeated measurements (Fig. 5b), and measurement time (Fig. 5c)—all had small non-significant effects on metabolic rate. Metabolic rates were higher in copepods sampled at Grønfjorden (ISG), the station most influenced by warm Atlantic water, compared to those sampled at Karlskronadjupet (ISK) in the middle of Isfjorden and Billefjorden (BAB), the innermost station with cold Arctic waters. Metabolic rates decreased with repeated measurements but increased as measurement time increased. Accounting for the effect of sampling station, repeated measurement and measurement time could be important for calculating partial regressions, so that the predictors of interest become more comparable, although in this particular case, these three variables had minimal effects on metabolic rates.

The adjusted R^2 values of models containing dry weight and species increased steadily from the start of the experiment, peaking just after 10 min (Fig. 6a). In contrast, models that included only temperature as a variable exhibited the opposite trend, with near-zero values up to 10 min, followed by a steady increase. After ∼10 min, the adjusted R^2 values for models containing dry weight and species (Fig. 6a and b) began to decline, while those for models including temperature (Fig. 6a and c) continued to rise. Thus, species and dry weight were more influential initially, whereas temperature became increasingly important as the measurement period progressed.

Discussion

This study compared the metabolic rates of high-latitude copepods of different body mass and life strategies to investigate the effects of increasing temperatures, ranging from 0°C to 6°C. Predicted temperature increases in the Arctic are expected to lead to smaller species becoming more dominant with cascading marine ecosystem impacts (Renaud et al. 2018, Møller and Nielsen 2020). Our findings on aerobic scope indicate that larger copepods have a greater fitness reduction with

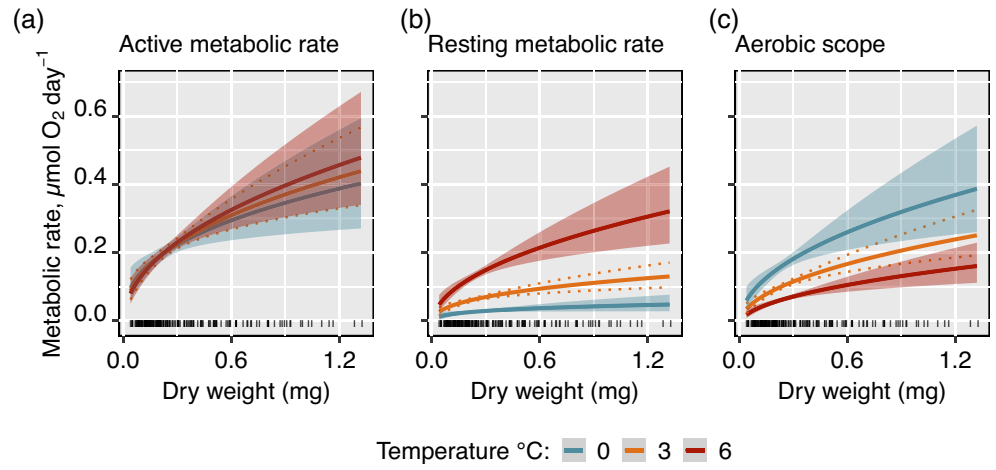

Figure 4. Model effects (partial regressions) from the three-way interaction between temperature, dry weight, and metabolic measurement for AMR (a), RMR (b), and aerobic scope (c). The 95% confidence intervals are represented as shaded ribbons for metabolic rates at 0°C and 6°C, and as dots for 3°C. Points along the *x*-axis indicate the dry weight of individual copepods. Partial regression predictions were calculated by setting the remaining predictors (i.e. all but temperature, dry weight, and metabolic measurement) to their average value (Fox and Weisberg 2018).

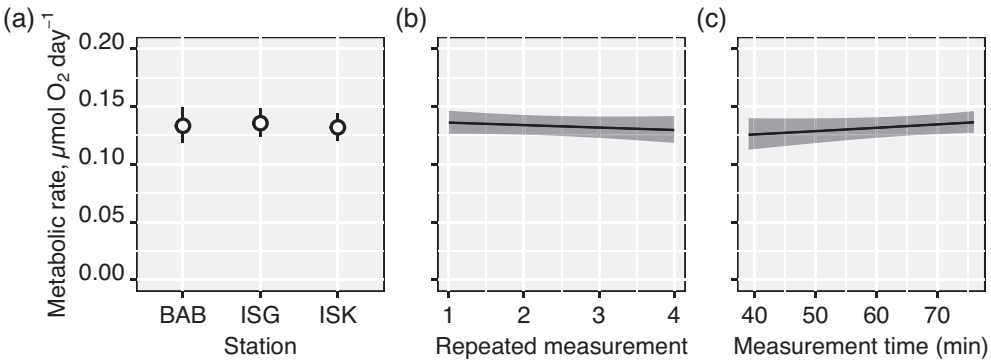

Figure 5. Model effects (partial regressions) of the three main effects: station (a), repeated measurement (b), and measurement time (c). In panel (a), station BAB represents Billefjorden, ISG represents Grønfjorden, and ISK represents Karlskronadjupet. The 95% confidence intervals are depicted as bars in (a) and as shaded ribbons in (b) and (c). Partial regression predictions were calculated by setting the remaining predictors (i.e. all but station, repeated measurement, and measurement time—within the respective panels) to their average value (Fox and Weisberg 2018).

rising temperatures than smaller ones. An effect that may be further amplified when considering other traits, such as the increased visibility of larger zooplankton to predators in an ice-free warmer environment that also accommodates more migratory fish predators (Langbehn and Varpe 2017). Factors that all increase the mortality risks of large-bodied zooplankton relative to smaller ones.

We found that while the AMR remained relatively stable across the temperature range, the RMR increased, leading to a decrease in aerobic scope with increased temperature. This pattern, which reflects a reduced energy budget for aquatic life in warmer waters, is also recognized by Rubalcaba et al. (2020). As temperatures rise from 0°C to 6°C, the oxygen saturation point decreases by 14%, from 349 to 300 μmol l^{-1}. Therefore, as temperatures increase, aquatic animals require more oxygen, even as it becomes less available. Although oxygen limitation is not generally an issue in Isfjorden (Saghravani et al. 2024), stratification caused by summer freshwater inputs from snow and ice melt can occur, particularly in sheltered fjords (Skogseth et al. 2020). For instance, Billefjorden (BAB), in the innermost part of Isfjorden, has a sill that prevents water mixing (Skogseth et al. 2020), which may lead to relatively low oxygen concentrations near the bottom. In contrast, the other two stations, Grønfjorden (ISG) and Karlskronadjupet (ISK), are likely well-oxygenated. Nevertheless, the oxygen levels at these stations remain well above the threshold for hypoxia in marine systems, which is 62.5 μmol l^{-1} or 2 mg l^{-1} (Diaz 2001). To exemplify, we can do a rough estimate based on the RMRs of the largest copepods, which ranged between 0.1 and 0.3 μmol O_2 day^{-1} in this study. A 100 l barrel of seawater saturated at 0°C could support ~6800 copepods for 2 weeks before hypoxia would occur assuming a metabolic rate of 0.3 μmol O_2 day^{-1}.

There are various ways to estimate the metabolic rates of copepods. Earlier "water bottle" experiments often relied on pooled measurements of multiple individuals per replicate, even for large adults (Ikeda et al. 2001). However, as technology advances, there is a growing shift toward measuring single individuals. Despite this progress, the metabolic rates of the earliest life stages, such as nauplii, remain too low to be estimated individually (e.g. Holmes-Hackerd et al. 2023). Differences in methodology and measurement units across studies make direct comparisons challenging (discussed in Holmes-Hackerd et al. 2023, Karlsson and Søreide 2023). Many

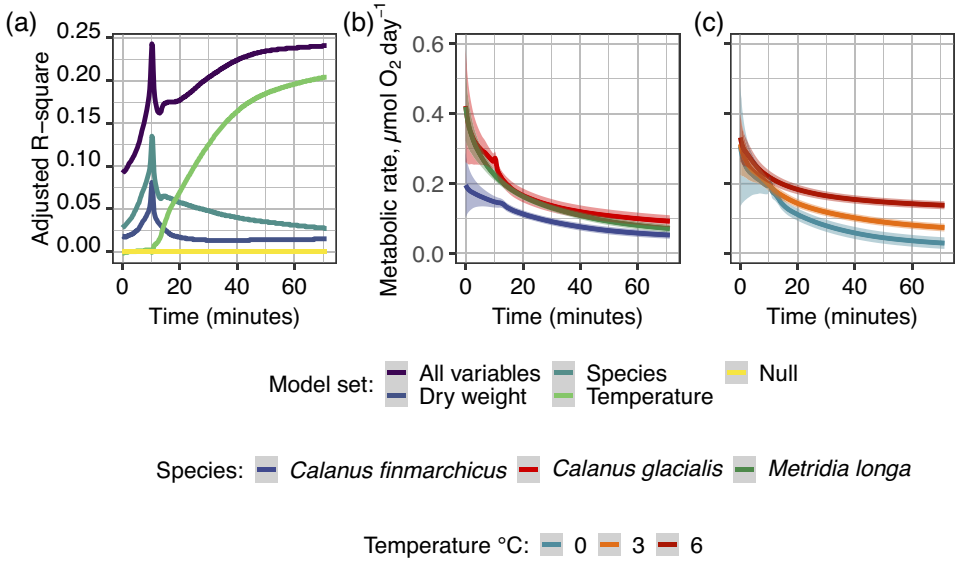

Figure 6. Panel (a) illustrates the adjusted R^2 values over time for five sets of models, each including one of the following: all variables (dry weight, species, and temperature), dry weight only, species only, temperature only, or intercept only (null model for reference). The measurement period encompasses 286 linear regression models, using rolling regression estimates of metabolic rate at time *i* as the response variable. Adjusted R^2 values were extracted from each model and plotted against time. Both metabolic rate and dry weight were log-transformed in these models. Panel (b) shows the average metabolic rate across species over time, while panel (c) shows the average rate across temperature over time. Shaded ribbons indicate 95% confidence intervals. For example, in panel (c), temperature curves initially overlap but progressively diverge over time. This pattern is reflected in panel (a), where the adjusted R^2 value for the model including temperature starts near zero and increases progressively. Conversely, panels (b) and (c) highlight the opposite trend for species, with species-related patterns diminishing over time. Note that in panel (b), rates of *C. glacialis* and *M. longa* are similar; meanwhile, they are different in Fig. 3. This is because *M. longa* is of considerable smaller size, and rates are not mass adjusted in panels (b) and (c), while they are in Fig. 3 which displays partial regressions.

studies report metabolic rates in carbon units, converting oxygen consumption to carbon using a respiratory quotient, due to the close relationship between oxygen consumption and carbon sequestration (Steinberg and Landry 2017).

For example, "water bottle" measurements compiled by Ikeda et al. (2001) reported oxygen consumption rates of 0.367, 0.482, and 0.466 μmol O_2 day^{-1} for females of *C. finmarchicus*, *C. glacialis*, and *M. longa*, respectively, at temperatures of 0°C, 2.3°C, and 0°C. These values are slightly higher than those found in our study, keeping in mind that rates may change due to temperature, season, methodology, and the copepods' life stage. In contrast, Ingvarsdóttir et al. (1999) reported *in situ* oxygen consumption rates for *C. finmarchicus* at 0°C in January at 0.094 μmol O_2 day^{-1}, which are more comparable to our findings. These values from Ikeda et al. (2001) and Ingvarsdóttir et al. (1999) were standardized by us to a copepod dry weight of 0.346 mg, which is the average mass of the copepods in our study, and was used for the predictions shown in Fig. 3.

Metridia longa exhibited a higher AMR than *C. finmarchicus* and *C. glacialis*. Similar results were observed in a previous experiment conducted during the polar winter, which also compared the metabolic rates of these species (Karlsson and Søreide 2023). This difference likely stems from the varying winter activities of these species, with *Calanus* spp. typically entering a resting state, while *M. longa* remains active and feeds opportunistically on the limited food available during winter (Hopkins et al. 1984, Gislason 2018, Jónasdóttir et al. 2019). Since this experiment was conducted during September and October, which in this region is the onset of the polar night, *Calanus* spp. was likely in its winter state (Freese et al. 2017, Hatlebakk et al. 2022). The visually inspected *Calanus* individuals had empty guts; meanwhile, *M. longa* occasionally had visible fragments of ingested particles. The *Calanus* species overwintering strategy of reduced activity is the key driver of the species distinct metabolic rates in this study. However, it is likely that all three species would have more similar AMRs if these experiments were conducted in spring. As spring initiates egg production and feeding in *Calanus* as well as *M. longa*, two functions known to greatly increase metabolic rates (Kiørboe et al. 1985, Morata and Søreide 2015).

When temperature increases, the RMR eventually reaches the AMR, and no energy is left for anything other than basic maintenance and survival (Pörtner and Farrell 2008, Rubalcaba et al. 2020). This occurs when the temperature rises to a point where the aerobic scope is zero and the animal can no longer cope. According to our results, the aerobic scope is greatest at 0°C and decreases as the temperature rises and was the lowest at 6°C. At 6°C, the copepods had not reached an aerobic scope that indicates that 6°C is dangerously high. In Isfjorden, where the copepods were sampled, surface temperatures rarely exceed 6°C and get progressively colder with depth (Skogseth et al. 2020).

For *C. glacialis* in waters off Svalbard, Alcaraz et al. (2014) identified 6°C as the upper thermal limit for functionality, beyond which survival becomes unlikely. Although we observed a reduction in fitness with increasing temperatures, our results neither confirm nor refute the findings of Alcaraz et al. (2014). Nevertheless, local populations of *C. glacialis* can be found in fjords along the Norwegian mainland, where temperatures exceed 6°C (Choquet et al. 2017). Similarly, *C. finmarchicus* is found in fjords on the Scottish west coast, where the entire water column sometimes exceeds 10°C, and these copepods

still accumulate fat deposits at such temperatures (Clark et al. 2012, Coguiec et al. 2023).

It is possible that the enclosed environment of fjords facilitates the local retention of well-adapted genotypes, thereby promoting the evolution of greater temperature tolerance than is typically found in oceanic populations. During summer, copepods migrate vertically, feeding and digesting food near the surface and seeking visual shelter at deeper depths. This behavior exposes them to a range of temperatures and allows copepods to regulate their physiology by moving through layers of water with different temperatures (McLaren 1963). Since AMR remains similar across temperatures, the temperature during feeding is less critical. Instead, the temperature when the copepod is at rest becomes more important, which copepods can regulate by descending from the surface to colder, deeper water. The temperature when the copepod is resting should preferably be cold, then the copepod can allocate more of its energy budget to building up fat and gonads and less to basic metabolism.

The *Calanus* species exhibit interspecific Bergmann clines, where body size increases progressively closer to the North Pole (Leinaas et al. 2016). Within species, body size also tends to increase with latitude (Choquet et al. 2018). In this study, we found that at 0°C, aerobic scope increases more steeply with body mass than at 6°C. This means that although larger individuals have a greater aerobic scope across all temperatures, the difference in scope between small and large individuals decreases as temperature rises. Therefore, being smaller becomes relatively more advantageous as temperature increases.

Since water temperature correlates with other parameters, such as oxygen and food availability, it is challenging to determine which factors influence body size in accordance with Bergmann clines. Whether temperature, oxygen, food seasonality, or a combination of these factors drives this size variation remains unclear (Allan 1976, Rubalcaba et al. 2020, Verberk et al. 2021). However, evidence tends to support temperature as the primary cause (Campbell et al. 2021). The species in this study inhabit open temperate and Arctic oceans, where oxygen deficiency is likely a minor issue. Therefore, temperature, combined with strong seasonality in food availability, is the most probable explanation for the Bergmann pattern of copepod size in these regions (e.g. Falk-Petersen et al. 2009, Renaud et al. 2018).

Time-specific analysis of metabolic data

From the analysis of metabolic rate, we observed that the AMR remained relatively stable across different temperatures. This pattern was also visible in the plot of temperature specific metabolic rates and adjusted R^2 values over time in Fig. 6a and c. Metabolic rates were highest at the beginning of the measurements when the copepods were agitated by the handling procedure (Karlsson and Søreide 2023). During this initial period, the explanatory power of dry weight and species was the highest, while temperature had little to no explanatory power. As the copepods calmed down, the importance of dry weight and species decreased by the same amount it initially increased. Meanwhile, temperature became progressively more important, as seen in the analysis of RMRs.

The rather slow initial increase in adjusted R^2 due to dry weight and species is likely a delayed response caused by the lack of mixing in the wells. By plotting adjusted R^2 against time, we can gain a better understanding of the events occurring within the sealed chambers during measurement. The consistently low R^2 values are likely due to the similar body size of most individuals and variation in activity levels, which may cancel out the effect of size. For instance, at a certain point in time, a small individual might be more active than a larger one, diminishing the expected size effect. A previous study found that activity level had a greater impact than body mass within a particular range of mass (Karlsson and Søreide 2023).

Summary and outlook

Our results provide mechanistic support for the observed shifts toward greater abundances of smaller boreal copepod species in the Arctic (Renaud et al. 2018, Møller and Nielsen 2020). Although larger individuals still possess greater aerobic scopes than smaller ones across our experimental temperature range of 0°C–6°C, they experience a relatively greater decrease in aerobic scope as temperature increases. Consequently, the ongoing warming of the Arctic diminishes the metabolic fitness advantages of being large. When considering that larger bodies are more easily seen and hence more susceptible to predation, combined with changing light conditions as sea ice retreats—creating better opportunities for visually hunting predators—the increased mortality risk for large-bodied copepods may become even more challenging. However, larger copepods can store relatively more fat, which may help them better endure the short food pulse during the summer and the long, unproductive Arctic winter. Food storage provides a crucial buffer, but in the long term, the presence of large copepods in a rapidly warming Arctic remains uncertain.

Acknowledgments

The authors would like to thank Maja Hatlebakk and Stuart Thomson for their assistance in the lab and Vanessa Pitusi for excellent fieldwork. The authors declare that all applicable international, national, and/or institutional guidelines for sampling, care, and experimental use of organisms for the study have been followed and all necessary approvals have been obtained. No approval of research ethics committees was required to accomplish the goals of this study because the experimental work was conducted with unregulated invertebrate species.

Author contributions

Both authors contributed to the study conception and design. K.K. performed the experiments, analyzed the data, and wrote the first draft of the manuscript, and J.S. commented on previous versions. Both authors read and approved the final manuscript.

Conflict of interest: None declared.

Funding

This research was part of the Nansen Legacy project funded by the Research Council of Norway (RCN # 276730). Additional funding was provided by the 2017–2018 Belmont Forum and BiodivERsA joint call, under the BiodivScen ERA-Net COFUND program to project ACCES (De-icing of the

Arctic Coast: critical or new opportunities for marine biodiversity) and from the European Union's Horizon 2020 research and innovation program under grant agreement number 869154 to project FACE-IT (The Future of Arctic Coastal Ecosystems—Identifying Transitions in Fjord Systems and Adjacent Coastal Areas).

Data availability

Data and code are available at https://doi.org/10.21335/NMDC-1073422505 and https://doi.org/10.5281/zenodo.14520445.

References

Alcaraz M, Felipe J, Grote U *et al.* Life in a warming ocean: thermal thresholds and metabolic balance of Arctic zooplankton. *J Plankton Res* 2014;**36**:3–10. https://doi.org/10.1093/plankt/fbt111

Allan JD. Life history patterns in zooplankton. *Am Nat* 1976;**110**:165–80. https://doi.org/10.1086/283056

Arnkværn G, Daase M, Eiane K. Dynamics of coexisting *Calanus finmarchicus*, *Calanus glacialis* and *Calanus hyperboreus* populations in a high-Arctic fjord. *Polar Biol* 2005;**28**:528–38. https://doi.org/10.1007/s00300-005-0715-8

Bates D, Maechler M, Bolker B *et al.* Fitting linear mixed-effects models using lme4. *J Stat Softw* 2015;**67**:1–48. https://doi.org/10.18637/jss.v067.i01

Bolker BM, Brooks ME, Clark CJ *et al.* Generalized linear mixed models: a practical guide for ecology and evolution. *Trends Ecol Evol* 2009;**24**:127–35. https://doi.org/10.1016/j.tree.2008.10.008

Burton T, Killen SS, Armstrong JD *et al.* What causes intraspecific variation in resting metabolic rate and what are its ecological consequences? *Proc R Soc B* 2011;**278**:3465–73. https://doi.org/10.1098/rspb.2011.1778

Campbell MD, Schoeman DS, Venables W *et al.* Testing Bergmann's rule in marine copepods. *Ecography* 2021;**44**:1283–95. https://doi.org/10.1111/ecog.05545

Chabot D, Steffensen JF, Farrell AP. The determination of standard metabolic rate in fishes. *J Fish Biol* 2016;**88**:81–121. https://doi.org/10.1111/jfb.12845

Choquet M, Hatlebakk M, Dhanasiri AK *et al.* Genetics redraws pelagic biogeography of *Calanus*. *Biol Lett* 2017;**13**:20170588. https://doi.org/10.1098/rsbl.2017.0588

Choquet M, Kosobokova K, Kwaśniewski S *et al.* Can morphology reliably distinguish between the copepods *Calanus finmarchicus* and *C. glacialis*, or is DNA the only way? *Limnol Oceanogr: Methods* 2018;**16**:237–52. https://doi.org/10.1002/lom3.10240

Clark KAJ, Brierley AS, Pond DW. Composition of wax esters is linked to diapause behavior of *Calanus finmarchicus* in a sea loch environment. *Limnol Oceanogr* 2012;**57**:65–75. https://doi.org/10.4319/lo.2012.57.1.0065

Clark TD, Sandblom E, Jutfelt F. Aerobic scope measurements of fishes in an era of climate change: respirometry, relevance and recommendations. *J Exp Biol* 2013;**216**:2771–82. https://doi.org/10.1242/jeb.084251

Coguiec E, Last KS, Cohen JH *et al.* Photoperiodism and overwintering in boreal and sub-Arctic *Calanus finmarchicus* populations. *Mar Ecol Prog Ser* 2023;**712**:49–65. https://doi.org/10.3354/meps14307

Daase M, Eiane K, Aksnes DL *et al.* Vertical distribution of *Calanus* spp. and *Metridia longa* at four Arctic locations. *Mar Biol Res* 2008;**4**:193–207. https://doi.org/10.1080/17451000801907948

Diaz RJ. Overview of hypoxia around the world. *J Environ Qual* 2001;**30**:275–81. https://doi.org/10.2134/jeq2001.302275x

Diel S. Zur lebensgeschichte dominanter Copepodenarten (*Calanus finmarchicus*, *C. glacialis*, *C. hyperboreus*, *Metridia longa*) in der Framstraße. *Ber Polarfor sch (Rep Polar Res)* 1991;**88**:1–118.

Falconer DS, Mackay TFC. *Introduction to Quantitative Genetics*, (4th edn). Harlow, Essex: Longman, 1996.

Falk-Petersen S, Mayzaud P, Kattner G *et al.* Lipids and life strategy of Arctic *Calanus*. *Mar Biol Res* 2009;**5**:18–39. https://doi.org/10.1080/17451000802512267

Fossen EI, Pelabon C, Einum S. Genetic and environmental effects on the scaling of metabolic rate with body size. *J Exp Biol* 2019;**222**:jeb193243. https://doi.org/10.1242/jeb.193243

Fox J, Weisberg S. Visualizing fit and lack of fit in complex regression models with predictor effect plots and partial residuals. *J Stat Softw* 2018;**87**:1–27. https://doi.org/10.18637/jss.v087.i09

Fox J, Weisberg S. *An R Companion to Applied Regression*, (3rd edn). Thousand Oaks, CA: SAGE Publishing, 2019.

Freese D, Søreide JE, Graeve M *et al.* A year-round study on metabolic enzymes and body composition of the Arctic copepod *Calanus glacialis*: implications for the timing and intensity of diapause. *Mar Biol* 2017;**164**:1–12. https://doi.org/10.1007/s00227-016-3036-2

Gabrielsen TM, Merkel B, Søreide JE *et al.* Potential misidentifications of two climate indicator species of the marine Arctic ecosystem: *C alanus glacialis* and *C. finmarchicus*. *Polar Biol* 2012;**35**:1621–8. https://doi.org/10.1007/s00300-012-1202-7

Gislason A. Life cycles and seasonal vertical distributions of copepods in the Iceland Sea. *Polar Biol* 2018;**41**:2575–89. https://doi.org/10.1007/s00300-018-2392-4

Gluchowska M, Kwasniewski S, Prominska A *et al.* Zooplankton in Svalbard fjords on the Atlantic–Arctic boundary. *Polar Biol* 2016;**39**:1785–802. https://doi.org/10.1007/s00300-016-1991-1

Griffith GP, Hop H, Vihtakari M *et al.* Ecological resilience of Arctic marine food webs to climate change. *Nat Clim Change* 2019;**9**:868–72. https://doi.org/10.1038/s41558-019-0601-y

Hagen W. Reproductive strategies and energetic adaptations of polar zooplankton. *Invertebr Reprod Dev* 1999;**36**:25–34. https://doi.org/10.1080/07924259.1999.9652674

Hatlebakk M, Niehoff B, Choquet M *et al.* Seasonal enzyme activities of sympatric *Calanus glacialis* and *C. finmarchicus* in the high-Arctic. *Front Mar Sci* 2022;**9**:877904. https://doi.org/10.3389/fmars.2022.877904

Fry FEJ. 1–The effect of environmental factors on the physiology of fish. In: WS Hoar, DJ Randall (eds), *Fish Physiology, Environmental Relations and Behavior*, Vol. **6**, New York, London: Academic Press, 1971;1–98. https://doi.org/10.1016/S1546-5098(08)60146-6

Holmes-Hackerd M, Sasaki M, Dam HG. Naupliar exposure to acute warming does not affect ontogenetic patterns in respiration, body size, or development time in the cosmopolitan copepod *Acartia tonsa*. *PLoS One* 2023;**18**:e0282380. https://doi.org/10.1371/journal.pone.0282380

Hopkins CCE, Tande KS, Grønvik S *et al.* Ecological investigations of the zooplankton community of Balsfjorden, Northern Norway: an analysis of growth and overwintering tactics in relation to niche and environment in *Metridia longa* (Lubbock), *Calanus finmarchicus* (Gunnerus), *Thysanoessa inermis* (Krøyer) and *T. raschi* (M. Sars). *J Exp Mar Biol Ecol* 1984;**82**:77–99. https://doi.org/10.1016/0022-0981(84)90140-0

Ikeda T, Kanno Y, Ozaki K *et al.* Metabolic rates of epipelagic marine copepods as a function of body mass and temperature. *Mar Biol* 2001;**139**:587–96. https://doi.org/10.1007/s002270100608

Ingvarsdóttir A, Houlihan DF, Heath MR *et al.* Seasonal changes in respiration rates of copepodite stage V *Calanus finmarchicus* (Gunnerus). *Fish Oceanogr* 1999;**8**:73–83. https://doi.org/10.1046/j.1365-2419.1999.00002.x

Jónasdóttir SH, Wilson RJ, Gislason A *et al.* Lipid content in overwintering *Calanus finmarchicus* across the subpolar eastern North Atlantic Ocean. *Limnol Oceanogr* 2019;**64**:2029–43. https://doi.org/10.1002/lno.11167

Jutfelt F, Norin T, Ern R *et al.* Oxygen-and capacity-limited thermal tolerance: blurring ecology and physiology. *J Exp Biol* 2018;**221**:jeb169615. https://doi.org/10.1242/jeb.169615

Karlsson K, Søreide JE. Linking the metabolic rate of individuals to species ecology and life history in key Arctic copepods. *Mar Biol* 2023;**170**:156. https://doi.org/10.1007/s00227-023-04309-x

Karlsson K, Winder M. Adaptation potential of the copepod *Eurytemora affinis* to a future warmer Baltic Sea. *Ecol Evol* 2020;**10**:5135–51. https://doi.org/10.1002/ece3.6267

Kiørboe T. How zooplankton feed: mechanisms, traits and trade-offs. *Biol Rev* 2011;**86**:311–39. https://doi.org/10.1111/j.1469-185X.2010.00148.x

Kiørboe T, Møhlenberg F, Hamburger K. Bioenergetics of the planktonic copepod *Acartia tonsa*: relation between feeding, egg production and respiration, and composition of specific dynamic action. *Mar Ecol Prog Ser* 1985;**26**:85–97. https://doi.org/10.3354/meps026085

Klekowski RZ, Węsławski JM. *Atlas of the Marine Fauna of South Spitsbergen, Invertebrates*, Vol. **2**, Gdansk: Ossolineum, 1991.

Langbehn TJ, Varpe Ø. Sea-ice loss boosts visual search: fish foraging and changing pelagic interactions in polar oceans. *Global Change Biol* 2017;**23**:5318–30. https://doi.org/10.1111/gcb.13797

Lefevre S. Are global warming and ocean acidification conspiring against marine ectotherms? A meta-analysis of the respiratory effects of elevated temperature, high CO_2 and their interaction. *Conserv Physiol* 2016;**4**:cow009. https://doi.org/10.1093/conphys/cow009

Leinaas HP, Jalal M, Gabrielsen TM *et al.* Inter-and intraspecific variation in body-and genome size in calanoid copepods from temperate and Arctic waters. *Ecol Evol* 2016;**6**:5585–95. https://doi.org/10.1002/ece3.2302

Lindmark M, Huss M, Ohlberger J *et al.* Temperature-dependent body size effects determine population responses to climate warming. *Ecol Lett* 2018;**21**:181–9. https://doi.org/10.1111/ele.12880

McKenzie DJ, Zhang Y, Eliason EJ *et al.* Intraspecific variation in tolerance of warming in fishes. *J Fish Biol* 2021;**98**:1536–55. https://doi.org/10.1111/jfb.14620

McLaren IA. Effects of temperature on growth of zooplankton, and the adaptive value of vertical migration. *J Fish Res Board Can* 1963;**20**:685–727. https://doi.org/10.1139/f63-046

Møller EF, Nielsen TG. Borealization of Arctic zooplankton—smaller and less fat zooplankton species in Disko Bay, Western Greenland. *Limnol Oceanogr* 2020;**65**:1175–88. https://doi.org/10.1002/lno.11380

Montero-Pau J, Gómez A, Muñoz J. Application of an inexpensive and high-throughput genomic DNA extraction method for the molecular ecology of zooplanktonic diapausing eggs. *Limnol Oceanogr: Methods* 2008;**6**:218–22. https://doi.org/10.4319/lom.2008.6.218

Morata N, Søreide JE. Effect of light and food on the metabolism of the Arctic copepod *Calanus glacialis*. *Polar Biol* 2015;**38**:67–73. https://doi.org/10.1007/s00300-013-1417-2

Morozov S, Leinonen T, Merilä J *et al.* Selection on the morphology–physiology-performance nexus: lessons from freshwater stickleback morphs. *Ecol Evol* 2018;**8**:1286–99. https://doi.org/10.1002/ece3.3644

Pante E, Simon-Bouhet B, Irisson J. 2023. marmap: import, plot and analyze bathymetric and topographic data. *R package version 1.0.10*, https://CRAN.R-project.org/package=marmap (3 May 2024, date last accessed).

Pebesma E, Bivand R. *Spatial Data Science: With Applications in R*. New York: Chapman and Hall/CRC, 2023. https://doi.org/10.1201/9780429459016

Pedersen T. 2023. patchwork: the composer of plots. *R package version 1.1.3*, https://CRAN.R-project.org/package=patchwork (19 December 2023, date last accessed).

Pörtner H. Climate change and temperature-dependent biogeography: oxygen limitation of thermal tolerance in animals. *Naturwissenschaften* 2001;**88**:137–46. https://doi.org/10.1007/s001140100216

Pörtner HO, Farrell AP. Physiology and climate change. *Science* 2008;**322**:690–2. https://doi.org/10.1126/science.1163156

Renaud PE, Daase M, Banas NS *et al.* Pelagic food-webs in a changing Arctic: a trait-based perspective suggests a mode of resilience. *ICES J Mar Sci* 2018;**75**:1871–81. https://doi.org/10.1093/icesjms/fsy063

Rubalcaba JG, Verberk WC, Hendriks AJ *et al.* Oxygen limitation may affect the temperature and size dependence of metabolism in aquatic ectotherms. *Proc Natl Acad Sci* 2020;**117**:31963–8. https://doi.org/10.1073/pnas.2003292117

Saghravani SR, Böttcher ME, Hong WL *et al.* *In situ* parameters, nutrients and dissolved carbon distribution in the water column and pore waters of Arctic fjords (Western Spitsbergen) during a melting season. *Earth Syst Sci Data* 2024;**16**:3419–31. https://doi.org/10.5194/essd-16-3419-2024

Scrucca L, Fraley C, Murphy TB *et al.* *Model-Based Clustering, Classification, and Density Estimation Using Mclust in R*. New York: Chapman and Hall/CRC, 2023. https://doi.org/10.1201/9781003277965

Seth H, Gräns A, Sandblom E *et al.* Metabolic scope and interspecific competition in sculpins of Greenland are influenced by increased temperatures due to climate change. *PLoS One* 2013;**8**:e62859. https://doi.org/10.1371/journal.pone.0062859

Skjoldal HR, Båmstedt U, Klinken J *et al.* Changes with time after capture in the metabolic activity of the carnivorous copepod *Euchaeta norvegica* Boeck. *J Exp Mar Biol Ecol* 1984;**83**:195–210. https://doi.org/10.1016/S0022-0981(84)80001-5

Skogseth R, Olivier LL, Nilsen F *et al.* Variability and decadal trends in the Isfjorden (Svalbard) ocean climate and circulation—an indicator for climate change in the European Arctic. *Prog Oceanogr* 2020;**187**:102394. https://doi.org/10.1016/j.pocean.2020.102394

Smolina I, Kollias S, Poortvliet M *et al.* Genome-and transcriptome-assisted development of nuclear insertion/deletion markers for *Calanus* species (Copepoda: Calanoida) identification. *Mol Ecol Resour* 2014;**14**:1072–9. https://doi.org/10.1111/1755-0998.12241

Søreide JE, Dmoch K, Blachowiak-Samolyk K *et al.* Seasonal mesozooplankton patterns and timing of life history events in high-Arctic fjord environments. *Front Mar Sci* 2022;**9**:933461. https://doi.org/10.3389/fmars.2022.933461

Steinberg DK, Landry MR. Zooplankton and the ocean carbon cycle. *Annu Rev Mar Sci* 2017;**9**:413–44. https://doi.org/10.1146/annurev-marine-010814-015924

UNESCO. *Monographs on Oceanographic Methodology: Zooplankton Sampling*. Paris: UNESCO, 1968.

Verberk WC, Atkinson D, Hoefnagel KN *et al.* Shrinking body sizes in response to warming: explanations for the temperature–size rule with special emphasis on the role of oxygen. *Biol Rev* 2021;**96**:247–68. https://doi.org/10.1111/brv.12653

Weydmann A, Walczowski W, Carstensen J *et al.* Warming of subarctic waters accelerates development of a key marine zooplankton *Calanus finmarchicus*. *Global Change Biol* 2018;**24**:172–83. https://doi.org/10.1111/gcb.13864

Wickham H. *ggplot2: Elegant Graphics for Data Analysis*. New York: Springer-Verlag, 2016

Zeileis A, Grothendieck G. zoo: S3 infrastructure for regular and irregular time series. *J Stat Softw* 2005;**14**:1–27. https://doi.org/10.18637/jss.v014.i06

Handling Editor: Ken Andersen